

STATISTICAL CHARACTERISTICS OF HARRIS CORNER DETECTOR

Umut Orguner and Fredrik Gustafsson

Department of Electrical Engineering
Linköping University
SE-581 83 Linköping, Sweden
{umut, fredrik}@isy.liu.se

ABSTRACT

In this study, a method is proposed to calculate the bias and mean square error matrix of Harris detector calculated corners. The main result is presented in a theorem and the performance of the algorithm is shown on an example.

Index Terms— Harris corner detector, bias, covariance, mean square error.

1. INTRODUCTION

Vision sensors as cameras are becoming standard sensors in many sensor fusion applications, as:

- Automotive collision avoidance algorithms [1], where vision information is being merged with radar and lidar sensors, for tracking surrounding vehicles and detecting stationary objects.
- Augmented reality applications [2], where inertial sensor information is supported with features detected in the image frames to prevent drift in dead-reckoning, and in the end provide accurate camera pose estimation and prediction.
- Airborne navigation and surveillance systems using for instance unmanned aerial vehicles, where the basic goal is the same as in augmented reality; to prevent drift in the navigation system.

A simple yet powerful algorithm to detect features in an image is the Harris detector [3]. As shown in [2], it gives real-time estimation of a large number of features, which can be tracked from frame to frame with classical target tracking algorithms [4, 5] for data association, track management and Kalman filtering. The only part that is missing to use the Harris detector in tracking and navigation applications as listed above is a reliable measure of uncertainty. It is the purpose of this contribution to provide an expression for bias and co-

variance¹ of the detected feature, that can be directly used in a Kalman filter based sensor fusion algorithm.

This document is organized as follows. Section 2 introduces our notation. The main result of the paper is given in Section 3 as a theorem and the performance of our algorithm is illustrated in Section 4. We finalize the paper with brief conclusions in Section 5.

2. THE HARRIS DETECTOR

2.1. Notation and definitions

Let $I(x, y)$ be a function of two spatial coordinates x and y . For black and white images $I \in \mathcal{R}^1$, while color images give $I \in \mathcal{R}^3$. Let

$$H(x, y) = \begin{pmatrix} \frac{\partial I^2}{\partial x^2} & \frac{\partial I^2}{\partial x \partial y} \\ \frac{\partial I^2}{\partial y \partial x} & \frac{\partial I^2}{\partial y^2} \end{pmatrix} \quad (1)$$

denote the Hessian of this function. The Harris operator based on $I(\cdot, \cdot)$ is defined as

$$\begin{aligned} R_I(x, y) &= \det(H(x, y)) - k(\operatorname{tr}(H(x, y)))^2 \\ &= \lambda_1 \lambda_2 - k(\lambda_1 + \lambda_2)^2, \end{aligned} \quad (2)$$

where λ_i are the two eigenvalues of the Hessian and k is an empirical scalar which is generally chosen in the interval $[0.04, 0.06]$. For color images where the function I is three-dimensional, the Harris operator can be generalized in different ways, see [6]. Most easily, the sum of $R(x, y)$ for each dimension can be used. Features are detected as

$$[\hat{x}, \hat{y}] = \arg \operatorname{local} \max_{x, y} |R(x, y)|. \quad (4)$$

Basically, the Harris detector works as follows:

- For a constant function, the Hessian is zero, and so is the Harris operator.
- For a pure gradient in the function, the Hessian has one non-zero and one zero eigenvalue, and the Harris operator becomes negative.

The authors gratefully acknowledge fundings from SSF (Swedish Foundation for Strategic Research) Strategic Research Center MOVIII and the Vinnova/FMV TAIS project ARCUS.

¹More rigorously, we must say the mean square error matrix. However, in this study, we will use the terms covariance and mean square error matrix interchangeably for the sake of simplicity.

- For two intersecting gradients (a “corner”), both eigenvalues are non-zero and the Harris operator is positive.

2.2. Numeric approximation

A true image $I^o(x, y)$ is measured subject to quantization and additive noise $\hat{I}[i, j] = I^o(x_i, y_j) + w[i, j]$ for $1 \leq i \leq N_x$ and $1 \leq j \leq N_y$. The partial derivatives in (1) can be approximated² as

$$\frac{\partial I^2}{\partial x^2} \approx \sum_{m,n} g[m, n] \hat{I}_x^2[i - m, j - n], \quad (5)$$

$$\frac{\partial I^2}{\partial x \partial y} \approx \sum_{m,n} g[m, n] \hat{I}_x[i - m, j - n] \hat{I}_y[i - m, j - n], \quad (6)$$

$$\frac{\partial I^2}{\partial y^2} \approx \sum_{m,n} g[m, n] \hat{I}_y^2[i - j, y - n] \quad (7)$$

where $g[\cdot, \cdot]$ is a weighting window with radius N_g and the gradient images are given using suitable derivative operators (e.g. Sobel operators etc.) $D_x[\cdot, \cdot]$ and $D_y[\cdot, \cdot]$ as

$$\hat{I}_x[i, j] = D_x[i, j] * \hat{I}[i, j] \quad \text{and} \quad \hat{I}_y[i, j] = D_y[i, j] * \hat{I}[i, j].$$

3. MAIN RESULT

Assumptions:

- Pixels of the noise image $w[\cdot, \cdot]$ are independent and identically distributed with a density function $w[i, j] \sim \mathcal{N}(0, \sigma_w^2)$ for all i and j .
- There is one and only one true corner in the vicinity of the Harris detector calculated corner estimate

$$[\hat{i}, \hat{j}] = \arg \text{local max}_{i,j} R_{\hat{I}}[i, j]. \quad (8)$$

- The local maximum of the cornerness map obtained using the true image $I^o[\cdot, \cdot]$ gives the true corner position i.e.,

$$[\hat{i}^o, \hat{j}^o] = \arg \text{local max}_{i,j} R_{I^o}[i, j]. \quad (9)$$

The main result can now be stated as follows.

Theorem 1 Suppose that we have obtained an estimate $[\hat{i}, \hat{j}]$ from the Harris corner detector; then, we define the bias and the covariance of this estimate as

$$\alpha_{m,n} = P \left\{ i_m = \hat{i}^o \& j_n = \hat{j}^o \right\} \quad (10)$$

$$\mu_{(\hat{i}, \hat{j})} \triangleq \begin{bmatrix} \hat{i} \\ \hat{j} \end{bmatrix} - \sum_{m,n} \alpha_{m,n} \begin{bmatrix} i_m \\ j_n \end{bmatrix} \quad (11)$$

$$\Sigma_{(\hat{i}, \hat{j})} \triangleq \sum_{m,n} \alpha_{m,n} \left(\begin{bmatrix} i_m \\ j_n \end{bmatrix} - \begin{bmatrix} \hat{i} \\ \hat{j} \end{bmatrix} \right) \left(\begin{bmatrix} i_m \\ j_n \end{bmatrix} - \begin{bmatrix} \hat{i} \\ \hat{j} \end{bmatrix} \right)^T \quad (12)$$

²The approximations here are correct up to a scaling factor.

where $i_m = \hat{i} + m$ and $j_n = \hat{j} + n$ and m, n ranges in the interval $[-N_p, N_p]$. Here, N_p is the radius of the region around the corner estimate $[\hat{i}, \hat{j}]$ in which the probabilities $\alpha_{m,n}$ that the pixel $[i_m, j_n]$ is the true corner will be calculated. The probability calculations are done as follows:

$$\alpha_{m,n} = \prod_l \text{normcdf} \left(\left(\frac{1}{\sigma_w} \bar{Q}_{m,n}^{-1} \bar{r}_{m,n} \right)_l \right) \quad (13)$$

where the l 'th element of a vector ξ is shown as $(\xi)_l$. In (13),

- The vector $\bar{r}_{m,n}$ is in \mathbb{R}^8 if $|m|, |n| \leq 1$ and in \mathbb{R}^9 otherwise. Its first 8 elements are formed

$$(\bar{r}_{m,n})_l \triangleq R_{\hat{I}}[i_m, j_n] - R_{\hat{I}}[i_u, j_v] \quad (14)$$

for integers u and v satisfying $-1 \leq u, v \leq 1$, and $|u| + |v| \neq 0$ where $i_u = i_m + u$ and $j_v = j_n + v$.³ Its 9th element (if any) is equal to

$$(\bar{r}_{m,n})_9 \triangleq R_{\hat{I}}[i_m, j_n] - R_{\hat{I}}[\hat{i}, \hat{j}] \quad (15)$$

- The size of the real positive definite matrix $\bar{Q}_{m,n}$ is 8×8 if $|m|, |n| \leq 1$ and 9×9 otherwise. It is the positive definite square root of $\bar{R}_{m,n} \bar{R}_{m,n}^T$ where $\bar{R}_{m,n}$ has 8 rows if $|m|, |n| \leq 1$ and 9 rows otherwise. Its first 8 rows are formed using elements of

$$\left[\frac{\partial R_{\hat{I}}[i_m, j_n]}{\partial I[s, t]} \Big|_{I=\hat{I}} - \frac{\partial R_{\hat{I}}[i_u, j_v]}{\partial I[s, t]} \Big|_{I=\hat{I}} \right]_{\substack{1 \leq s \leq N_x \\ 1 \leq t \leq N_y}} \quad (16)$$

for the same $[u, v]$ pairs as in (14). Its 9th row (if any) is formed of the elements of⁴

$$\left[\frac{\partial R_{\hat{I}}[i_m, j_n]}{\partial I[s, t]} \Big|_{I=\hat{I}} - \frac{\partial R_{\hat{I}}[\hat{i}, \hat{j}]}{\partial I[s, t]} \Big|_{I=\hat{I}} \right]_{\substack{1 \leq s \leq N_x \\ 1 \leq t \leq N_y}} \quad (17)$$

- $\text{normcdf}(\cdot)$ is the cumulative distribution function of a univariate Gaussian random variable with zero mean and unity variance.

Proof: Omitted in this draft version.

4. EXAMPLE

In this section, we are going to calculate the covariance and bias of the corners on a test image. For this purpose the Harris corner detector as described above, which uses Sobel operators for the derivatives and takes $k = 0.4$, is executed and the local maxima of the cornerness map which have cornerness

³There are a total of 8 $[u, v]$ pairs which satisfy these inequalities. These correspond to 8 neighbors of $[i_m, j_n]$.

⁴Calculation of the partial derivatives $\frac{\partial R_{\hat{I}}[i_m, j_n]}{\partial I[s, t]}$ of the cornerness measure at point $[i_m, j_n]$ with respect to intensity of the pixel $[s, t]$ is straightforward and not added here due to space limitations.

value greater than the threshold 10^5 are selected to be the corner estimates. Then the covariance and bias estimates are calculated for each detected corner. The radius of the probability calculation area around a corner is selected as $N_p = 4$ pixels. Once all $(2 \times 4 + 1)^2 = 81$ probabilities are calculated they are normalized so that the normalized probabilities sum up to unity⁵. The covariance and bias are then calculated using the normalized probabilities which represent an approximate density for the true corner. The smoothing window $g[.,.]$ is a Gaussian window of standard deviation set to 1 pixel with radius $N_g = 3$ pixels. The standard deviation σ_w of the noise on the image is assumed to be 20. The results are illustrated in Figure 1. The red(green, blue) + signs denote the corner positions detected by the Harris detector in the red(green, blue) component of the image. The corresponding · signs and ellipses illustrate the bias compensated (i.e., expected) corner positions and 99% confidence regions calculated using the covariance estimates of our algorithm respectively. Figure

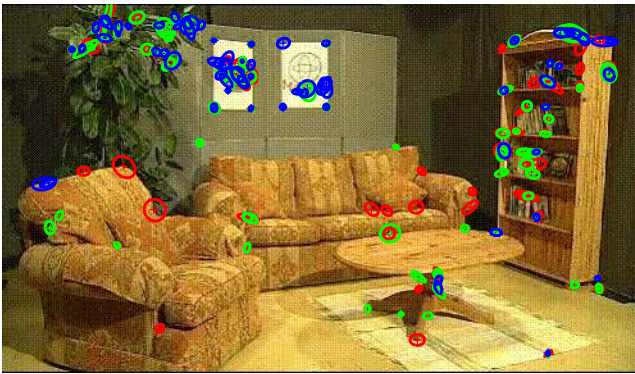


Fig. 1. Covariances (%99 confidence region ellipses), expected (· signs) and detected (+ signs) corners in the red green and blue components of the image [2].

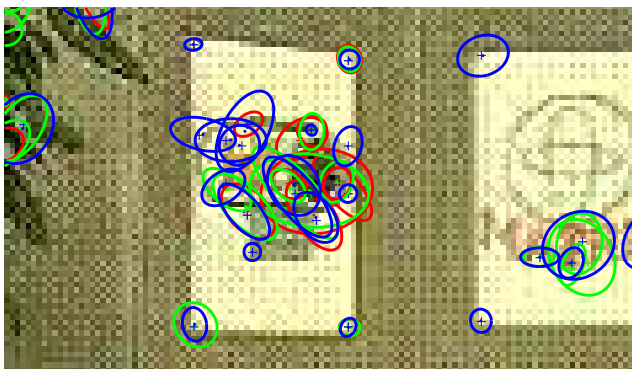


Fig. 2. Zoomed version of Figure 1.

⁵This normalization amounts to a conditioning of the probabilities by the event that the true corner is in the area where the probabilities are calculated.

2 shows the middle top part of Figure 1 zoomed. It is apparent here that, the obvious corners of picture on the wall are represented by “small” covariances whereas the detected corners inside the pictures are assigned large uncertainties due to the fact that the cornerness map around those points are fluctuating significantly to allow nearby points to get selected as corners with almost equal chance. This increases the bias calculated by our algorithm and makes the components of the covariance in the direction of the bias grow. It is also remarkable for Figure 2 that the covariance and bias estimates can vary for different (red green or blue) components of the image. The magnitude of the calculated uncertainty representations therefore can be used to select the component of the image that gives less uncertainty (e.g. for tracking purposes).

5. CONCLUSIONS

Uncertainty descriptions for Harris corner detector are defined and a method is proposed to calculate them. Our work is specialized to the cornerness measure of (3), however it is straightforward to apply the same framework to other cornerness measures as well. Moreover, it is possible to generalize the method to correlated noise processes as long as the second order statistics of any noise vector \bar{w} which is formed from the elements of the noise image $w[.,.]$ is supplied.

6. REFERENCES

- [1] F. Gustafsson, “Challenges in signal processing for automotive safety systems (plenary paper),” in *IEEE Statistical Signal Processing Workshop*, Bordeaux, 2005, IEEE.
- [2] J. Chandaria, G. Thomas, B. Bartczak, K. Koeser, R. Koch, M. Becker, G. Bleser, D. Stricker, C. Wohlleber, M. Felsberg, F. Gustafsson, J. Hol, T.B. Schön, J. Skoglund, P.J. Slycke, and S. Smeitz, “Real-time camera tracking in the MATRIS project,” in *Proceedings of International Broadcasting Convention*, Amsterdam, September 2006, IEE.
- [3] C. Harris and M.J. Stephens, “A combined corner and edge detector,” in *4th Alvey Vision Conference*, Manchester, UK, 1988, pp. 147–151.
- [4] Y. Bar-Shalom and X. R. Li, *Estimation and Tracking: Principles, Techniques, and Software*, Artech House, Norwell, MA, 1993.
- [5] Y. Bar-Shalom and X. R. Li, *Multitarget Multisensor Tracking: Principles and Techniques*, YBS Publishing, Storrs, CT, 1995.
- [6] M. Felsberg and G.H. Granlund, “POI detection using channel clustering and the 2D energy tensor,” in *Pattern Recognition: 26th DAGM Symposium*, Tübingen, Germany, 2004, vol. 3175 of *LNCS*, pp. 103–110, Springer Berlin.